A method to measure the hyperelastic parameters of *ex vivo* breast tissue samples

2004 Phys. Med. Biol. 49 4395

(http://iopscience.iop.org/0031-9155/49/18/014)

INSTITUTE OF PHYSICS PUBLISHING PHYSICS IN MEDICINE AND BIOLOGY

Phys. Med. Biol. **49** (2004) 4395–4405 PII: S0031-9155(04)77438-2

A method to measure the hyperelastic parameters of *ex vivo* breast tissue samples

Abbas Samani[1] **and Donald Plewes**[2]

[1] Department of Medical Biophysics/Electrical and Computer Engineering, University of Western Ontario, London, ON N6A 5C1, Canada
[2] Department of Medical Biophysics, University of Toronto, 2075 Bayview Avenue, Toronto, ON M4N 3M5, Canada

E-mail: asamani@uwo.ca

Received 10 March 2004
Published 3 September 2004
Online at stacks.iop.org/PMB/49/4395
doi:10.1088/0031-9155/49/18/014

Abstract

Over the past decade, there has been increasing interest in modelling soft tissue deformation. This topic has several biomedical applications ranging from medical imaging to robotic assisted telesurgery. In these applications, tissue deformation can be very large due to low tissue stiffness and lack of physical constraints. As a result, deformation modelling of such organs often requires a treatment, which reflects nonlinear behaviour. While computational techniques such as nonlinear finite element methods are well developed, the required intrinsic nonlinear mechanical parameters of soft tissues that are critical to develop reliable tissue deformation models are not well known. To address this issue, we developed a system to measure the hyperelastic parameters of small *ex vivo* tissue samples. This measurement technique consists of indenting an unconfined small block of tissue using a computer controlled loading system while measuring the resulting indentation force. The nonlinear tissue force–displacement response is used to calculate the hyperelastic parameters via an appropriate inversion technique. This technique is based on a nonlinear least squares formulation that uses a nonlinear finite element model as the direct problem solver. The features of the system are demonstrated with two samples of breast tissue and typical hyperelastic results are presented.

(Some figures in this article are in colour only in the electronic version)

1. Introduction

The mechanical properties of soft tissues are of increasing interest for various medical applications such as computer-assisted interventional procedures and medical imaging. There

are numerous examples in the former case where tissue deformation models play a major role. In brain surgery, the brain deforms as a result of force and boundary condition alterations. Such alterations can result from opening the skull or change in the head position and rotation during surgery. This deformation can render pre-surgery images useless for intra-operative applications. As such these images must be updated to guide surgeons through surgery. Miga *et al* (1999) developed a finite element (FE) model where they calculated brain deformation resulting from the brain's gravity load to update MRI images taken prior to surgery. Samani and Plewes (2002) presented a nonlinear FE model to calculate breast tissue deformation. The purpose of this model was to update data of breast MRI images taken in prone position to more accurately reflect the supine breast during surgery. Medical imaging registration is another application in which tissue deformation modelling has been recently utilized. As an alternate approach to conventional non-rigid registration techniques such as mutual information-based techniques (Rueckert *et al* 1999), Samani *et al* (2001) proposed FE-based model for breast non-rigid image registration while Schnabel *et al* (2003) used the FE-based approach to validate breast non-rigid image registration. More recently, a number of investigators have proposed FE models for soft tissue mechanical simulation of tissue cutting and needle insertion. Such models are helpful in developing image guided intervention techniques and virtual reality environments used for training. Cotin and Delingette (1998) proposed a simplified FE model based on a superposition principle and pre-computation for surgery simulation. To simulate needle insertion, DiMaio and Salcudean (2002) developed a linear elastic FE model, which calculates tissue deformation and force distribution along needle shaft during insertion. While the FE method has been well known to simulate tissue deformation with reasonable accuracy, its fidelity strongly depends on the accuracy of the mechanical properties used in the FE models.

Elastography is a novel imaging technique that has emerged over the past decade for imaging soft tissue elastic modulus (Ophir *et al* 1991, Muthupillai *et al* 1995, Chenevert *et al* 1998, Plewes *et al* 2000). These methods use elastic modulus reconstruction techniques with a linear elastic tissue deformation model as their direct solver component. Van Houten *et al* (2003) summarized the elastic modulus of breast tissues obtained by a number of elastography studies and showed considerable variation in elastic modulus values obtained for each tissue type. Moreover, Varghese *et al* (2000) used simulated ultrasound (US) elastograms to investigate the impact of the nonlinear behaviour of breast tissues on the diagnostic value of breast US elastograms and demonstrated that this nonlinearity has a significant impact on the elastographic contrast. Thus, more information regarding the constitutive properties of normal and abnormal tissues is needed to aid in the interpretation of current approaches to elastography. In an attempt to account for geometrical nonlinearity in elastography, Skovoroda *et al* (1999) presented a 2D elasticity reconstruction model for plain strain case. In an interesting paper, Sinkus *et al* (2002) used MR elastography to show evidence that various breast tissue pathologies exhibit different nonlinear mechanical characteristics. Moreover, Sack *et al* (2004) used a harmonic elastography technique to characterize the nonlinear behaviour of agarose gel. Using the quasi-static elastography approach, Samani *et al* (2003b) presented a constrained reconstruction algorithm to reconstruct the hyperelastic properties of breast tissues. This suggests that there is a potential for the development of nonlinear elastography techniques with higher specificity than traditional linear elastography techniques. Since elastography techniques use tissue deformation models as their direct problem solvers, such techniques require nonlinear behaviour considerations in their direct problem component.

While the demand for nonlinear tissue parameters is high, surprisingly, there has been very little research done to measure them *in vitro* or *in vivo*. Using uniaxial and biaxial tests on *ex vivo* soft tissues such as the skin and ureteral muscle, they have been shown

to exhibit very significant nonlinear behaviour (Fung 1993). Similar nonlinear behaviour was shown for arterial walls using pressure–diameter and uniaxial testing on *ex vivo* animal arteries (Humphry 1995). Using uniaxial stretching tests, Maksym and Bates (1997) observed nonlinear behaviour of *ex vivo* tissue strips obtained from dog lungs. They developed models with distributed constituent properties to fit the measured stress–strain data. Krouskop *et al* (1998) measured the Young's modulus of 142 breast tissue and 113 prostate tissue *ex vivo* specimens under various compression levels, and noted that the modulus values increase significantly as a result of increasing the precompression load. While acknowledging the observed tissue nonlinear behaviour, no attempt was made to characterize the nonlinear behaviour and infer the underlying parameters in a systematic way. The fact that the tissue modulus is sensitive to the precompression load has implications to elastography in that some form of precompression is applied in addition to the mechanical stimulation. Given that tissue can exhibit nonlinear mechanical behaviour, this precompression and mechanical excitation amplitudes can introduce a confounding factor in data interpretation. This may explain some of the inconsistency in the data compiled by van Houten *et al* (2003). To characterize tissue nonlinear behaviour, Wellman (1999) developed a technique to measure the nonlinear elastic parameters of breast tissues using force–displacement data of thin slice tissues undergoing indentation experiment. To obtain the tissue Young's modulus values as a function of the indentation nominal strains, Wellman (1999) derived an approximate 1D analytical expression assuming exponential stress–strain relation.

The goal of this work is to provide a measurement method and preliminary data for breast tissue nonlinear parameters. Towards this end, we have developed a tissue indentation measurement technique to acquire the force–displacement response of small blocks of breast tissues. In this paper, we describe an inversion technique to infer the hyperelastic parameters of breast tissues. The technique uses a nonlinear least squares formulation with a 3D nonlinear FE model as its forward problem model. The measured parameters can be readily used in nonlinear FE tissue deformation models. Lastly, we conclude with discussion of plans for obtaining data set of various breast tissues that can be incorporated reliably in FE tissue deformation models required for relevant medical applications.

2. Theory

2.1. Finite deformation formulation

In order to model breast tissue deformation, it is imperative to use a finite deformation formulation of elasticity where the geometry change in the tissue is assumed to be significant. Under static conditions, the equilibrium equations governing the tissue are

$$\sum_{j=1}^{3} \frac{\partial \sigma_{ij}}{\partial x_j} + f_i = 0; \qquad i = 1, 2, 3 \tag{1}$$

where σ_{ij} represents components of the stress tensor and f_i denotes the body forces. For strain definition, the deformation gradient $F = \partial x/\partial X$ is defined where the current position of point p is $x = X + u$ in which X and u are the reference position of point p and its displacement, respectively. Using $B = F \cdot F^{\mathrm{T}}$, the strain invariants are defined as follows (Atkin and Fox 1980):

$$\begin{aligned} I &= \mathrm{tr}(B) \\ I_2 &= \tfrac{1}{2}\left(I_1^2 - \mathrm{tr}(B \cdot B)\right) \\ I_3 &= \det(F). \end{aligned} \tag{2}$$

A constitutive equation for isotropic hyperelastic tissue undergoing finite strains can be obtained based on a selected strain energy function $U(I_1, I_2, I_3)$. We idealize breast tissues as isotropic incompressible material. For such material, there are a number of strain energy functions such as the Neo-Hooke and polynomial forms (Spencer 1980) and the Arruda Boyce form (Arruda and Boyce 1993) that can be selected. The polynomial form is broadly used in modelling rubbers, which can be simplified for tissue modelling as follows:

$$U = \sum_{i+j=1}^{N} C_{ij}(I_1 - 3)^i (I_2 - 3)^j \tag{3}$$

in which $N = 2$ is the most commonly used in rubber modelling, C_{ij} represents the hyperelastic parameters which characterize the intrinsic nonlinear elastic behaviour of the tissue. The strain energy in equation (3) unlike some other models such as Ogden model, depends on the strain invariants I_1 and I_2 while it is independent of I_3. This implies that the breast tissue is isotropic and incompressible, which is consistent with the underlying assumptions in this work. The first two terms in this equation form a well-known Mooney–Rivlin energy function developed for incompressible rubbers. This energy form was used by Miller and Chinzei (1997) to measure the hyperelastic properties of brain tissue. It is the goal of this work to present a method for identifying these parameters using an indentation measurement technique. Based on the strain energy function U, the constitutive equation required for tissue deformation modelling can be obtained as follows (Holzapfel 2000):

$$\sigma = \frac{2}{\sqrt{I_3}}\left[\left(\frac{\partial U}{\partial I_1} + I_1\frac{\partial U}{\partial I_2}\right)B - \frac{\partial U}{\partial I_2}B.B + I_3\frac{\partial U}{\partial I_3}I\right] \tag{4}$$

where σ is the true stress tensor and I is the identity matrix. To calculate tissue displacements equations (1) through (4) must be solved simultaneously. This is done numerically using the FE method (Bathe 1996).

2.2. Inverse problem

The problem of tissue hyperelastic parameter calculation from force–displacement data obtained from tissue indentation experiment can be classified as an inverse problem. The goal here is to find a set of hyperelastic parameters such that the difference between the measured and calculated force–displacement response is minimum. The force $F_c(C_{ij})$ is a function of the hyperelastic parameters C_{ij}, and can be calculated using a nonlinear FE model given the known indentation profile. The FE model represents a nonlinear function relating the forces $F_c(C_{ij})$ resulting from tissue indentation simulation to the unknown hyperelastic parameters C_{ij}. Moreover, given that the linear elastic moduli of breast tissues are better known, mathematical constraints relating C_{ij} parameters can be added reflecting estimated values of the elastic modulus in the initial linear elastic behaviour of the tissue. As a result, this problem can be classified as a constrained nonlinear least squares problem as follows:

$$\begin{aligned} &R(C_{ij}) = F_e - F_c(C_{ij}) \qquad f(C_{ij}) = \tfrac{1}{2}R^T(C_{ij}) \cdot R(C_{ij}) \\ &\text{minimize } f(C_{ij}) \qquad \text{subject to } L_l \leqslant L(C_{ij}) \leqslant L_u. \end{aligned} \tag{5}$$

Here F_e represents the experimental force data, $L(C_{ij})$ is a linear operator and L_l and L_u are the lower and upper bounds of L, respectively. If a polynomial strain energy function (equation (3)) is used, given that $E = 6(C_{10} + C_{01})$ for incompressible materials, the following constraints can be used:

$$E_l \leqslant 6(C_{10} + C_{01}) \leqslant E_u \tag{6}$$

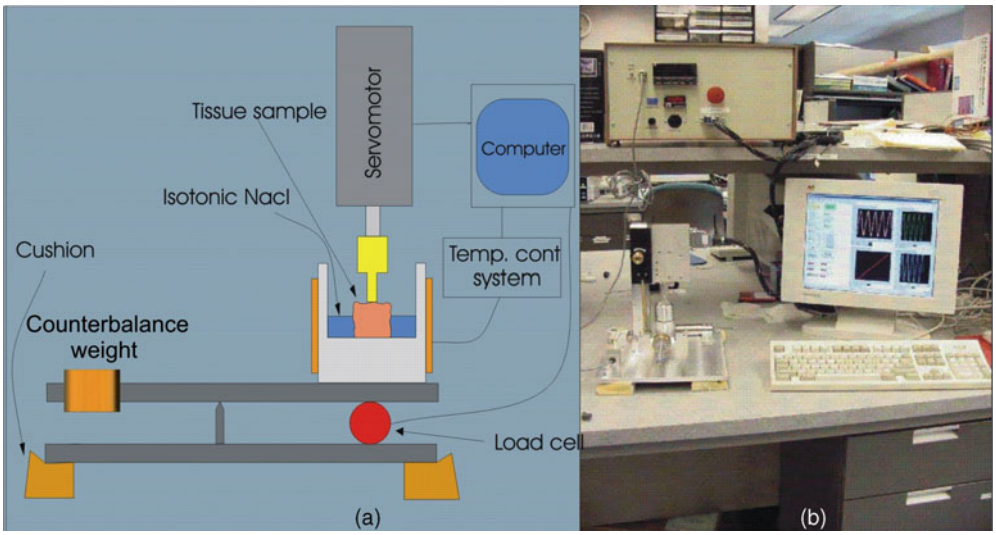

Figure 1. Tissue indentation measurement system. (a) Schematic of the tissue indentation apparatus and (b) photograph of apparatus.

where E_l and E_u are the lower and upper bound estimates of the tissue Young's modulus. To solve the constrained least-squares problem (5), Schittkowski (1988) developed an efficient technique by introducing a simple variable transformation which leads to a standard constrained minimization problem that can be solved using sequential quadratic programming (SQP) methods (Schittkowski 1988).

3. Materials and methods

3.1. Indentation test experimental set-up

To measure the hyperelastic parameters of breast tissues, a measurement system was developed that indents an unconstrained block of the tissue while measuring the resulting forces. For tissue indentation, the loading apparatus used by Samani *et al* (2003), which was developed to measure breast tissue elastic modulus, was used. This apparatus, which is shown in figure 1, is a custom-made electro-mechanical machine that consists of a programmable high resolution linear servo actuator LAL30 (SMAC, Carlsbad, CA, USA) for tissue actuation. The range motion of this actuator is 25 mm with 0.5 μm resolution and 1 μm accuracy. This actuator was controlled by a 6K2 motor controller (Parker Hannifin Corporation, Rhonert Park, CA, USA). For force measurement, an LC601-5 load cell (Omega Engineering Inc, Stamford, CT, USA) with a capacity of 5 lb was used. To maintain the tissue biological temperature throughout the experiment, a bench top Csi32 temperature control unit (Omega Engineering Inc, Stamford, CT, USA) was used to maintain a temperature of 37 °C to within ±0.1 °C. As shown in figure 1, the load cell was mounted underneath a pivoted solid platform where the sample holder is placed. This plate was attached to a rod with sliding weight to offset the weight of the plate and sample holder. The latter is required to obtain a near zero load cell reading which is necessary to allow the load cell to operate within its design dynamic range. The servo actuation system and the load cell were controlled by a computer (PC) via a LabVIEW program. The servo motor was driven by the 6K2 control unit through an RS232

serial port which communicates the LabVIEW program commands that specify the actuation profile to the control unit. The force acquisition unit includes an amplifier to amplify the load cell signal and an analog input card NI 6020E (National Instruments, Austin, TX, USA) used to sample the amplified load cell signal at a frequency of 1000 samples/s. The LabVIEW program controls the tasks of preloading the tissue sample, driving the servo motor for tissue indentation and finally sampling and storing the force and displacement data. The temperature control Csi32 unit consists of a thermal element glued to the exterior surface of the sample holder and a small thermal probe immersed in a thin layer of saline surrounding the tissue specimen.

3.2. Sample preparation and measurement protocol

Breast tissue specimens obtained from women who underwent breast reduction surgery were obtained and transported to the measurement lab within two hours after the surgery. By gross inspection, one specimen was identified as adipose tissue while the other was identified as fibroglandular tissue. From each sample, a $15 \times 15 \times 10$ mm^3 block shape specimen was cut using a cutting device developed for this purpose. As described in Samani *et al* (2003a), starting by freehand cutting, a tissue sample slightly larger than the desired $15 \times 15 \times 10$ mm^3 block was cut. This was then embedded in agarose in a transparent cylinder with orthogonal slits. The tissue was constrained within the cylinder to minimize tissue motion and deformation while being cut. The sample was then cut with a sharp blade guided by the orthogonal slits. The resulting specimens were cut to a dimension of $15 \times 15 \times 10$ mm^3 and then released from the cutting assembly. The resultant specimens may still undergo slight deformation as a result of their own weight load. In order to compensate for this, the new dimension of each specimen was measured and recorded. These dimensions were later used in the FE model required for hyperelastic parameter calculation. During loading, the tissue specimens were placed in a sample holder with a thin layer of saline for maintaining moisture and biological temperature. To start the loading experiment, a 5 mm diameter plane ended indenter connected to the servomotor was manually lowered and approximately positioned in contact with the centre of the sample's top surface. The servomotor was programmed to generate a sinusoidal motion with amplitude, frequency and number of cycles defined by the user via the LabVIEW program. For tissue preconditioning, the preload was set to 0.5 g and indentation amplitude, frequency and number cycles were set to 1.0 mm, 0.1 Hz and 25, respectively. After preconditioning with 25 cycles of sinusoidal indentation, the number of cycles was set to 5 for which the force–displacement data were acquired and recorded for offline processing.

3.3. Data inversion technique

To calculate the hyperelastic parameters of the tissue specimens, the force–displacement experimental data obtained from the indentation test were inverted using an inversion technique. This technique is summarized in the flowchart depicted in figure 2. The technique is based on the optimization problem (5) described in the theory section. In this problem F_e is the experimental force data and F_c represents corresponding forces resulting from simulating the indentation test using a nonlinear 3D FE model. Given the very low frequency of 0.1 Hz used in the experiment, static loading simulation was used to generate F_c. Furthermore, in equation (4), $N = 2$ was used which leads to five unknown parameters to be identified. The optimization problem (5) was formulated and solved using Schittkowski (1988) SQL technique. For the FE forward modelling, ABAQUS (Hibbit, Karlsson, Sorenson, Inc) was used in which the

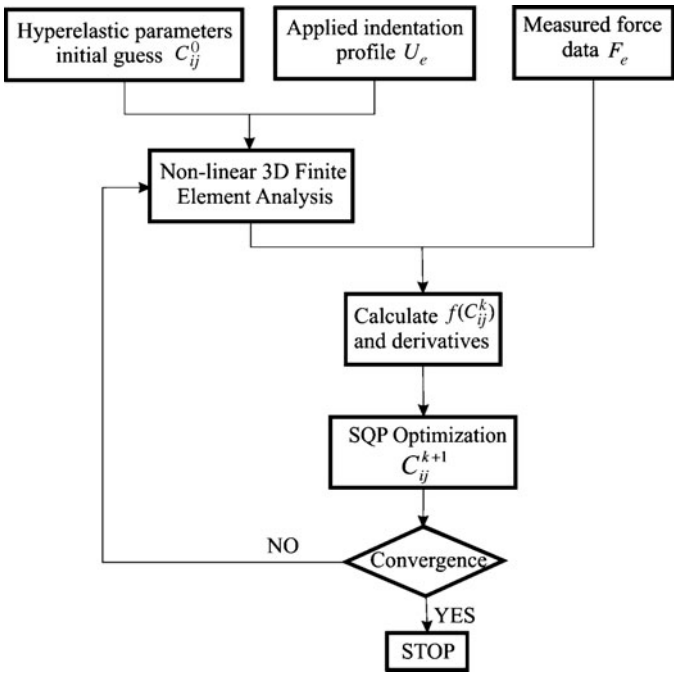

Figure 2. Flow chart of the computational unconstrained least squares inversion procedure used to calculate the tissue hyperelastic parameters from the measured force–displacement data.

tissue was modelled as hyperelastic material undergoing finite deformation. To calculate F_c using this FE model, friction between the tissue specimens and the sample holder was ignored. Furthermore, 1 mm indentation was applied to the central area of specimens while no friction between the indenter and specimens was considered. To implement this nonlinear inversion process, a MATLAB code was developed that invokes ABAQUS iteratively to obtain the residual function $R(C_{ij})$ in the inverse problem (5). The derivatives of this function with respect to the variables C_{ij} required in the SQL process were calculated using finite difference approximations.

4. Results

To demonstrate the performance of the presented measurement technique, we illustrate the data from two specimens obtained from breast reduction surgery procedures. These specimens were obtained from 26 and 34 year old females. By gross inspection, the specimens were identified to be adipose and fibroglandular tissues, respectively. After conducting the experiment, pathological examinations confirmed that the specimens were composed of over 85% of adipose and fibroglandular tissues, respectively. These specimens were cut into the required $15 \times 15 \times 10\,\text{mm}^3$ blocks and each block was tested at least four times to ensure measurement repeatability. After applying low frequency sinusoidal loading as described in the methods, the force–displacement data were obtained. The curves corresponding to the last loading cycle of the adipose tissue specimen are shown in figure 3. The upper and lower portions of this cycle represent the loading and unloading steps of the sinusoidal indentation. Throughout the unloading step, there are time windows where the indenter is not in contact with the

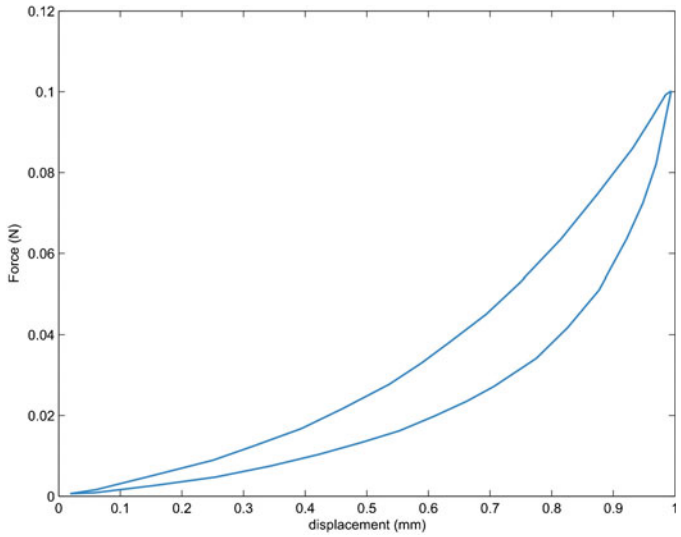

Figure 3. Plot of the force–displacement data obtained from the last indentation cycle of the adipose tissue.

Table 1. Calculated means and standard deviations of hyperelastic parameters for adipose and fibroglandular breast tissue specimens using a polynomial strain energy function with $N = 2$.

	(C_{10}	C_{01}	C_{11}	C_{20}	C_{02}) $\times 10^{-4}$ N mm^{-2}
Adipose tissue	3.1 ± 0.3	3.0 ± 0.2	22.5 ± 3	38.0 ± 6	47.2 ± 7
Fibroglandular tissue	3.3 ± 0.4	2.8 ± 0.3	44.9 ± 8	77.2 ± 11	94.5 ± 13

specimen due to the tissue viscoelasticity. During those windows, the force data reflected only experimental noise. Incorporating these signals with the data recorded while the indenter contact was established leads to unrealistically low force measurements. As such it was decided that the unloading portion be ignored in calculating the hyperelastic parameters. Using the loading portion of the cycle as a representative of the force data (F_e), the constrained nonlinear least squares-based inversion algorithm discussed in the methods was used to calculate the hyperelastic parameters of the tissue specimens. The optimization algorithm used to fit the data in this technique was stable but slowly convergent. Moreover, adding the linear constraints of equation (6) was fairly effective in improving numerical convergence. Figure 4 shows the loading portion of the indentation cycle with a solid line. This figure also depicts the force–displacement curve corresponding to an initial guess of the adipose tissue hyperelastic parameters in addition to the curve corresponding to the calculated parameters. The latter curve is in good agreement with the observed force–displacement curve. Finally the calculated means and standard deviations of hyperelastic parameters of the two adipose and fibroglandular tissue specimens are presented in table 1. In this table, C_{10} and C_{01} indicate that the Young's modulus of the tested tissue specimens is 3.6 KPa. This is consistent with the results obtained from our study of measuring the elastic modulus of ~200 breast tissue samples to be published in the near future. Higher order hyperelastic parameters indicate that, under higher strains, the fibroglandular tissue is stiffer than the adipose tissue. The same was observed by both Krouskop *et al* (1998) and Wellman (1999).

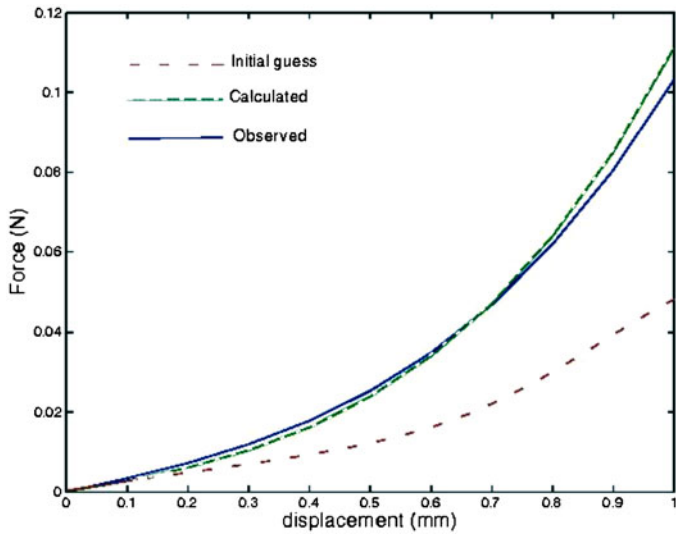

Figure 4. Three plots of the adipose tissue force–displacement curves demonstrating the calculation of its hyperelastic parameters. The measured data are shown by the solid line while data corresponding to initial guess and final solution of the hyperelastic parameters are shown by (– –) and (– – –), respectively.

5. Discussion and conclusions

In Samani *et al* (2003a), we described a system that was developed for measuring the Young's modulus of breast tissues using small block shape specimens. This paper extends our previous work to characterize the nonlinear behaviour of breast tissues. Given the low stiffness of breast tissues, the breast usually experiences large deformation while undergoing medical procedures such as imaging and surgery. Furthermore, similar to other biological soft tissues, breast tissues are known to be intrinsically nonlinear. As such reliable breast tissue deformation modelling requires that nonlinear mechanical behaviour arising from both large deformation and intrinsic mechanical nature be taken into account. Moreover, evidence has emerged recently (Sinkus *et al* 2003) which suggests that imaging breast tissue nonlinear elastic parameters may be specific to breast cancer. To extend our previous research to the measurement of the hyperelastic parameters of *ex vivo* breast tissue, we used a similar measurement apparatus to actuate small block shape tissue specimens to induce large deformation required to capture their hyperelastic parameters.

To calculate the hyperelastic parameters using the experimental force–deformation data, a constrained nonlinear least squares inverse problem was formulated and solved. The essence of this formulation was to find a set of hyperelastic parameters that minimizes the difference between the measured and simulated data. The forward problem solver in this formulation used to generate the simulated data was a 3D nonlinear FE model. In this model, we used the polynomial form of equation (3) to represent the strain energy function. This model is consistent with underlying isotropy and incompressibility assumptions used to idealize breast tissues in this work. Furthermore, this polynomial form resulted in a good fit for the measured force–displacement data as shown in figure 4.

The experiment was designed in such a way that errors related to boundary conditions uncertainties are minimal. For this purpose, the specimens were tested with as fewer constraints

as possible. To assess the impact of uncertainties related to the sample's bottom boundary conditions, we conducted numerical experiments for both samples using fixed supported bottom boundaries. We found that the hyperelastic parameters increased less than 15% with C_{01} and C_{10} increasing less than 6% compared to the unconstrained boundary. However, as illustrated in section 3.2, the tissue specimens were placed in the sample holder with a thin layer of saline throughout the experiment. This layer acts as a lubricant that provides a slippery surface, which decreases friction between the sample's bottom and sample holder. As such the unconstrained boundary assumed at the specimens' bottom constitutes a better approximation. To measure the hyperelastic parameters of tissues reliably, it is desirable that the tissue be loaded in such a way that many stress components are present throughout the specimen's volume. Unlike in conventional uniaxial experiments where only one uniformly distributed stress component is present, intuition confirmed by FE simulation of indenting small block shape specimens indicates that all stress components are present and thus more reliable measurement that can be used in simulating tissues under realistic loading conditions is anticipated.

In our measurement, the indentation amplitude was limited to 1 mm, which implies an average compressional strain of 10%. FE simulation, however, indicates that a maximum normal strain of over 15% is present in the specimen due to stress non-uniform distribution. This means that the hyperelastic parameter results obtained from our experiments are less reliable where strains higher than 15% are anticipated. The 1 mm indentation amplitude limit was imposed because we observed that plane ended indenters leave permanent damage to tissue specimens when significantly higher amplitudes were used. To avoid this problem and thus to obtain hyperelastic parameters appropriate for a wider range of deformation, spherical indenters can be used for tissue indentation. Moreover, the measured data in the presented technique represent the mechanical behaviour exhibited by the tissue after the preload is applied. Prior to applying the sinusoidal loading, the tissue specimens undergo the loading of their own weight followed by the preloading applied to establish a full contact between the indenter and specimen. This means that the initial portion of the force–displacement curve representing the tissue mechanical behaviour under small strains is missing. It is expected, however, that the impact of this missing data will be insignificant in both modelling breast tissue deformation and in elastography techniques where hyperelastic parameters are imaged.

The measurement results of the two tissue specimens discussed in this research were presented to demonstrate the feasibility of measuring the hyperelastic properties of breast tissues using the proposed technique. Further work and statistical analysis is required to measure the hyperelastic parameters of various types of breast tissues to obtain a hyperelastic parameter database that can be used in reliable breast tissue deformation simulation. Although the focus of this research is the hyperelastic properties of breast tissue, the proposed technique can be applied for other biological soft tissues such as the prostate or liver.

Acknowledgments

This study was supported under grants from the US Army breast Cancer Programme (DAMB17-99-1-9391), The Canadian Institute of Health Research and the Terry Fox Foundation of the National Cancer Institute of Canada.

References

Arruda E M and Boyce M C 1993 A three-dimensional constitutive model for the large stretch behavior of rubber elastic materials *J. Mech. Phys. Solids* **41** 389–412

Atkin R J and Fox N 1980 *An Introduction to the Theory of Elasticity* (London: Longman)

Bathe K-J 1996 *Finite Element Procedures in Engineering Analysis* (Englewood Cliffs, NJ: Prentice-Hall)

Chenevert T L, Skovoroda A R, O'Donnell M and Emelianov S Y 1998 Elasticity reconstructive imaging by means of stimulated echo MRI *Magn. Reson. Med.* **39** 482–90

Cotin S and Delingette H 1998 Real time surgery simulation with haptic feedback using finite elements *Proc. ICRA*

DiMaio S P and Salcudean S E 2002 Needle insertion modelling for the interactive simulation of percutaneous procedures *Proc. MICCAI*

Fung Y C 1993 *Biomechanics: Mechanical Properties of Living Tissues* (New York: Springer)

Holzapfel G A 2000 *Nonlinear Solid Mechanics* (Chichester: Wiley)

Humphrey J D 1995 Mechanics of the arterial wall: review and directions *Crit. Rev. Biomed. Eng.* **23** 1–162

Krouskop T A, Wheeler T M, Kallel F, Garra B S and Hall T 1998 Elastic moduli of breast and prostate tissues under compression *Ultrason. Imaging* **20** 260–74

Maksym G N and Bates J H T 1997 A distributed nonlinear model of lung tissue elasticity *J. Appl. Physiol.* **82** 32–41

Miga M I, Paulsen K D, Lemery J M, Eisner S D, Hartov A, Kennedy F E and Roberts D W 1999 Model-updated image guidance: initial clinical experiences with gravity-induced brain deformation *IEEE Trans. Med. Imaging* **18** 866–74

Miller K and Chinzei K 1997 Constitutive modelling of brain tissue. Experiment and theory *J. Biomech.* **30** 1115–21

Muthupillai R, Lomas D J, Rossman P J, Greenleaf J F, Manduca A and Ehman R L 1995 Magnetic resonance elastography by direct visualization of acoustic strain waves *Science* **269** 1854–7

Ophir J, Cespedes I, Ponnekanti H, Yazdi Y and Li X 1991 A quantitative method for imaging the elasticity of biological tissues *Ultrason. Imaging* **13** 111–34

Plewes D B, Bishop J, Samani A and Sciarretta J 2000 Visualization and quantification of breast cancer biomechanical properties with magnetic resonance elastography *Phys. Med. Biol.* **45** 1591–610

Rueckert D, Sonoda L I, Hayes C, Hill D L G, Leach M O and Hawkes D J 1999 Nonrigid registration using free-form deformations: applications to breast MR images *IEEE Trans. Med. Imaging* **18** 712–21

Sack I, MacGowan C, Samani A, Luginbuhl C, Oakden W and Plewes D B 2004 Observation of nonlinear shear wave propagation using magnetic resonance elastography MRM (at press)

Samani A, Bishop J, Luginbuhl C and Plewes D B 2003a Measuring the elastic modulus of *ex-vivo* small tissue samples *Phys. Med. Biol.* **48** 2183–98

Samani A, Bishop J, Yaffe M J and Plewes D B 2001 Biomechanical 3D finite element modeling of the human breast using MRI data *IEEE Trans. Med. Imaging* **20** 271–9

Samani A and Plewes D B 2002 Finite element model of MRI image updating for breast surgery *OCITS Workshop: Computational and Numerical Modeling for Image-guided Therapy and Surgery (Toronto)*

Samani A, Sack I and Plewes D B 2003b Constrained nonlinear elasticity reconstruction technique for breast MRI elastography *Proc. ISMRM 11th Annual Meeting* p 773

Schittkowski K 1988 Solving constrained nonlinear least squares problems by a general purpose SQP method *Trends in Mathematical Optimization* (Basle: Birkhauser)

Schnabel J A, Tanner C, Castellano-Smith A D, Degenhard A, Leach M O, Hose D R, Hill D L G and Hawkes D J 2003 Validation of non-rigid image registration using finite element methods: application to breast MR images *IEEE Trans. Med. Imaging* **22** 238–47

Sinkus R, Weiss S, Wigger E, Lorenzen J, Dargatz M and Kuhl C 2002 Nonlinear elastic tissue properties of the breast measured by MR-elastography: initial *in-vitro* and *in-vivo* results *Proc. ISMRM 10th Annual Meeting* 33

Skovoroda A R, Lubinski M A, Emelianov S Y and O'Donnell M 1999 Reconstructive elasticity imaging for large deformations *IEEE Trans. Ultrason. Ferroelectr. Freq. Control* **46** 523–35

Spencer A J M 1980 *Continuum Mechanics* (London: Longman)

van Houten E E W, Doyley M M, Kennedy F E, Weaver J B and Paulsen K D 2003 Initial *in vivo* experience with steady-state subzone-based MR elastography of the human breast *J. Magn. Reson. Imaging* **17** 72–85

Varghese T, Ophir J and Krouskop T A 2000 Nonlinear stress-strain relationships in tissue and their effect on the contrast-to-noise ratio in elastograms *Ultrasound Med. Biol.* **26** 839–51

Wellman P S 1999 Tactile imaging *PhD Thesis* Harvard University